

Frequency doubling in SBN crystals with random ferroelectric domains in the thermal focusing regime

Robert Fischer¹, Solomon M. Saitiel^{1,2}, Dragomir N. Neshev¹, Wieslaw Krolikowski³,
Alexander Dreischuh^{1,2}, and Yuri S. Kivshar¹

¹Nonlinear Physics Centre and Centre for Ultrahigh-bandwidth Devices
for Optical Systems (CUDOS), Research School for Physical Sciences and Engineering
Australian National University, Canberra, ACT 0200, Australia

²Faculty of Physics, Quantum Electronics Department, University of Sofia
5 J. Bourchier boulevard, BG-1164, Sofia, Bulgaria

³Laser Physics Centre and Centre for Ultrahigh-bandwidth Devices
for Optical Systems (CUDOS), Research School for Physical Sciences and Engineering
Australian National University, Canberra, ACT 0200, Australia

ABSTRACT

We consider the femtosecond phase-matched noncollinear second-harmonic generation (SHG) in Strontium Barium Niobate (SBN) crystals with random ferroelectric domains. We study both planar and radial second-harmonic (SH) radiation for the average input power P_f up to 600 mW. We show that the effect of thermal self-focusing of the fundamental wave occurring at $P_f > 250$ mW results in novel effects including the spatial localization of SHG, a change of the SH efficiency slope, and significant spectral broadening of both fundamental and SH beams.

Keywords: Second harmonic generation, Thermal focusing, Self-phase modulation, Cross phase modulation.

1. INTRODUCTION

Unpoled Strontium Barium Niobate (SBN) crystals are used in nonlinear optics as a nonlinear structured medium that allows a phase-matched second-harmonic generation (SHG) practically in the whole range of the crystal transparency^{1,2} without alignment, temperature tuning or poling. This is a great advantage with respect to other types of quadratic

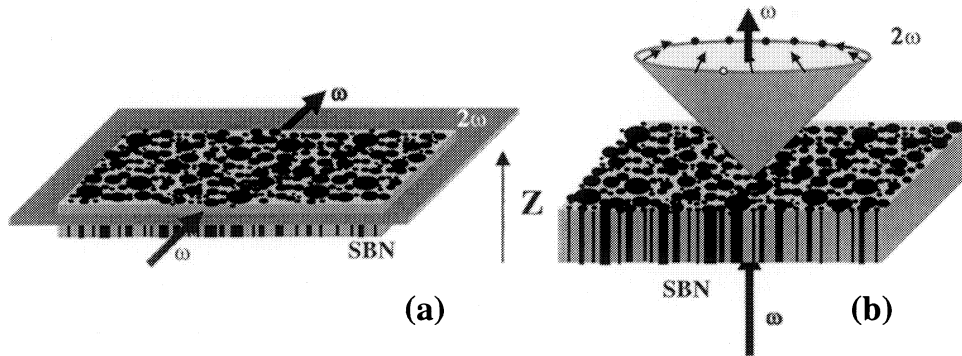


Fig. 1. Two geometries employed for the observation of self-matched SHG in a SBN crystal with random domain distribution for (a) plane shaped SH, and (b) ring-shaped SH .

S. M. Saitiel's e-mail: saitiel@phys.uni-sofia.bg

nonlinear media where special methods for the phase-matching are required, including birefringence or two-dimensional poling structures. Frequency independent self-phase matching in SBN crystal is due to a random distribution (in size and position) of anti-parallel ferroelectric domains (AFD). The needle-like AFD are orientated along the z-axis of the crystal, and thus they create a two-dimensional nonlinear photonic structure with a constant linear refractive index but randomly modulated nonlinear quadratic response. According to Ref. 3, the size of domains varies between 2 μm and 8 μm providing an infinite set of the grating vectors \mathbf{g} located in the (x,y) plane. In this way, the SHG phase matching (PM) condition $\mathbf{k}_2 = 2\mathbf{k}_1 + \mathbf{g}$ is fulfilled, where \mathbf{k}_1 and \mathbf{k}_2 are the wave vectors of the fundamental and second-harmonic waves, respectively. These PM conditions result in the SH radiation emitted in a plane when the fundamental wave is directed perpendicularly to z axis [see Fig. 1(a) and the insets in Fig. 3(a)] or as a cone [see Fig. 1(b) and the inset in Fig 3(b)] when the fundamental wave is directed along z axis. Unfortunately, the major advantage of the crystals with random AFD, i.e. *self-phase matching* in extremely broad spectral region, corresponds to lower conversion efficiency, and the development of methods for increasing the SHG efficiency will broaden possible applications of the SBN crystals with random AFD.

In this paper we demonstrate experimentally that thermally-induced self-focusing of the fundamental wave leads to a four-fold increase of the SHG efficiency generated by random domains of SBN. We also discuss how this effect changes other parameters of the SH radiation.

2. EXPERIMENTAL RESULTS AND DISCUSSIONS

For SHG, we use a femtosecond Ti:Sapphire oscillator (Mira, Coherent) emitting 150 fs (FWHM) pulses of 6 – 7 nJ energies at the repetition rate of 76 MHz, tunable in the range 700 – 900 nm. The laser beam (with an average power up to 550 mW) is focused inside the $5 \times 5 \times 10$ mm SBN:60 crystal by a lens of a 50 mm focal length. The focal spot size is measured to be 74 μm (FWHM). All sides of the SBN crystal have been polished allowing the observation of the SH radiation from different directions. The properties of the laser and SH pulses are characterized using spectrometer (HR2000, Ocean Optics) and FROG system (Grenouille-Model 8-50, Swamp Optics). The power of the fundamental and the SH radiation is measured with a power meter (Ophir). Estimated light intensity in the focal spot is about 1 GW/cm^2 . The peak power of a single pulse is less than the critical power for self-focusing due to electronic nonlinearity of the SBN crystal⁴.

At low average input powers, the divergence of the fundamental beam after its propagation in the SBN crystal is defined by the focal spot (~ 6.5 mrad@100 mW), whereas its spectral width is inversely proportional to the pulse duration (~ 70 cm^{-1} @100 mW). At high average powers, we observe an enhancement of the beam divergence (34 mrad@450 mW) and the broadening of the beam spectra (~ 150 cm^{-1} @550 mW). In order to clarify the origin of the nonlinearity that triggers these changes of the fundamental wave, i.e. thermal or electronic, we use a chopper in front of the SBN crystal to control the mean input power while keeping the light intensity unchanged. In this way, we decrease both the beam divergence and its spectral width that is direct indication of the thermal origin of the self-focusing of the fundamental wave inside the volume of the SBN crystal. This is illustrated in Fig. 2 where the SH spectra are measured with chopper “on” and “off”. The measured SH spectra are almost precise copies of the fundamental-beam spectra as shown in Ref. 2, so a direct comparison for the fundamental spectral width can be done. This observation clearly indicates that at the initial stage of the formation of an effective nonlinear lens is mediated by local heating of the crystal due to two-photon absorption of the fundamental beam. It is followed by the self-phase modulation of the fundamental beam due to the Kerr nonlinearity. The spectral width of the fundamental radiation increases and, after being replicated by the SH process, it results in an increased spectral width of the SH signal. Figures 3(a,b) show the efficiency of the SHG process as a function of the input power for two different geometries, namely, when the fundamental vector is perpendicular to the axis z, i.e. $[\mathbf{k}_1 \perp z]$, and when the fundamental vector is parallel to the axis z, $[\mathbf{k}_1 \parallel z]$. In the first case, the input polarization is chosen to be parallel to the z-axis. In the second case, the SHG process is independent on the orientation

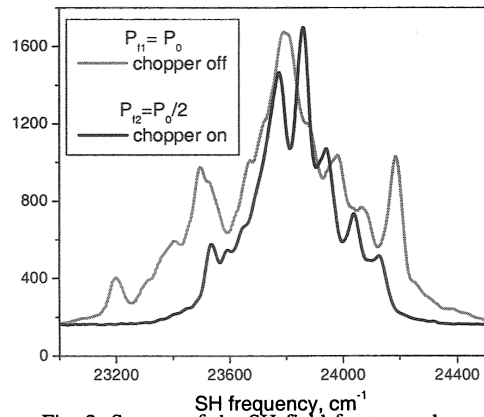


Fig. 2. Spectra of the SH field for two values of the average power but the same intensity.

of the fundamental polarization. In both the plots of Fig. 3 the change of the slope from linear to quadratic at the input power of 200-250mW is clearly visible. Linear dependence is what is expected for the conversion efficiency of the pure quadratic process, and it takes place at lower powers. The image marked with "LP" is recorded from the side of the SBN crystal; it demonstrates that the SH wave scattering in the perpendicular direction is constant, and it does not depend on the distance traveled by the fundamental beam.

This is in accord with the prediction for strongly noncollinear SHG, and it has the behavior similar to SHG in crystals with strong birefringence.

At higher powers, thermal self-focusing of the fundamental beam occurs leading to the appearance of a special region with much higher SH efficiency [see the inset in Fig. 3(a) marked as "HP"] coinciding with a new position of the focused fundamental beam. In this case, the increased intensity in the focal region compensates for the decreased length of the beam waist which length is inversely proportional to the input power. The net result is 3-fold increase of the SH efficiency for the planar geometry $[\mathbf{k}_1 \perp z]$ and 4-fold increase of the SH efficiency for the radial (cone) geometry $[\mathbf{k}_1 \parallel z]$.

In Fig. 4, we show the effect of thermal focusing on the divergence of the SH ring. Increasing the power leads to a reduction of the ring divergence as can be expected from the fact that the SH ring passes through a nonlinear lens. At low powers, the calculated angles

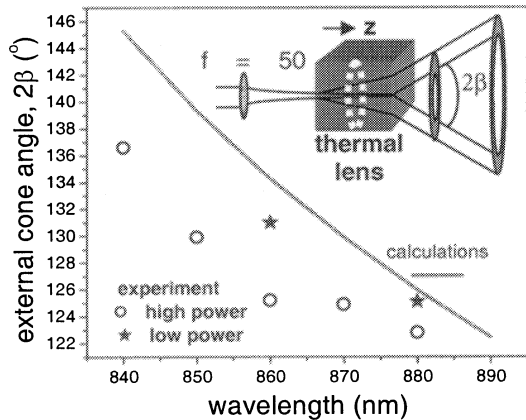


Fig.4. Divergence of the ring-shaped SH against the fundamental wavelength for high and low powers.

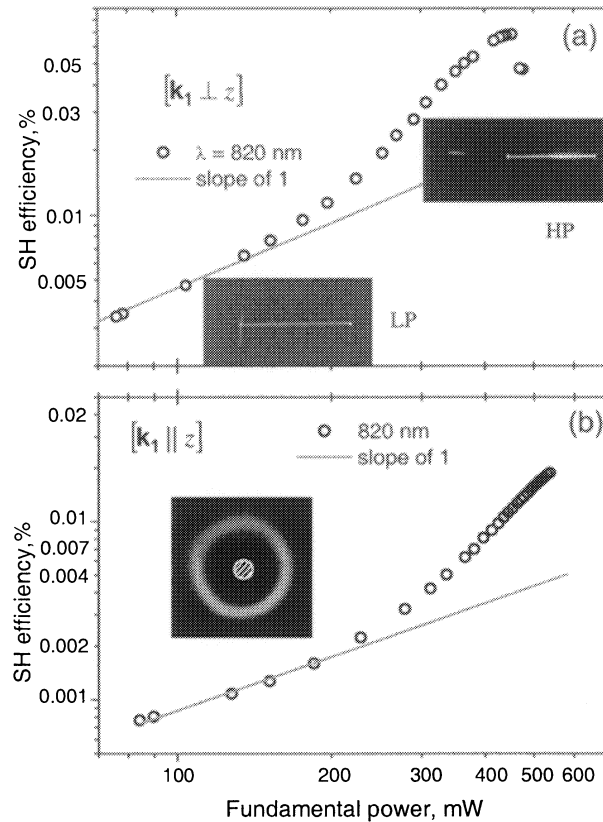


Fig. 3 . Efficiency of the SHG process for the two geometries $^{\perp}$ - (a)-and $^{\parallel}$ - (b) a function of the input power. Insets are photo of SH radiation. HP –high power; LP – low power.

of the external SHG cone are close to the theoretically values calculated from the longitudinal phase-matching condition $k_{2e} \cos \beta_0 = 2k_{10}$. Internal cone angle β_0 is obtained by solving numerically the equation $n_e(\lambda_2, \beta_0) \cos \beta_0 = n_o(\lambda_1)$ and knowing β_0 ; the external angle is determined from the Snell's law $\beta = \arcsin[n_e(\lambda_2, \beta_0) \sin \beta_0]$, where n_e and n_o are the wavelength dependent extraordinary and ordinary indices of refraction.

Another key property of the ring-shaped SH radiation in SBN crystals with random AFD is the radial polarization¹; see Fig. 5(a). So far no quantitative analysis of this effect has been reported in the literature. In our study, we investigate the contrast ratio for a part of the ring with a limited angular width. First, we assume that in an infinitely small angular sector of the ring the SH radiation is perfectly linearly polarized with the direction along the radius. Then, if we record with an analyzer the SH light from the angular sector with the width 2γ the normalized SH signal will be:

$$I_\gamma = \frac{1}{2\gamma} \int_{-\gamma}^{\gamma} \cos^2(x - \alpha) dx = \frac{1}{8\gamma} [\sin(2\gamma + 2\alpha) + \sin(2\gamma - 2\alpha) + \gamma],$$

where α is the analyzer rotational angle. Then the extinction polarization ratio is a function of the angular sector width 2γ and it is expressed as follows: $E_r = I_\gamma(\alpha = \pi/2)/I_\gamma(\alpha = 0)$

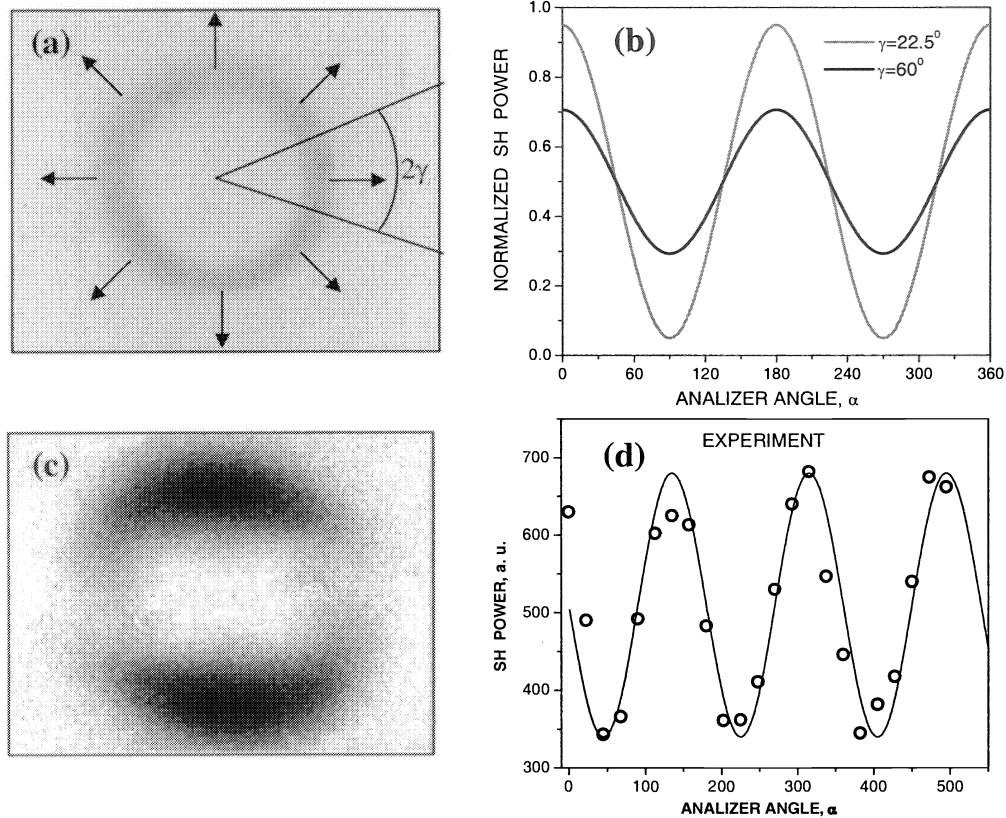


Fig. 5. (a) Experimental image of the SH ring taken without an analyzer. The definition of collecting angle γ is indicated. The arrows illustrates the radial polarization property; b) theoretical polarization analyzing curve for two values of the collecting angle γ : 22.5° and 60° ; c) experimental photo of the SH ring taken with analyzer; d) experimental polarization analyzing curve for $\gamma = 22.5^\circ$.

In Fig. 5(b) we plot the theoretical dependences for I_γ for two values of the collecting angle γ , 22.5° and 60° . The ring-shaped SH after the analyzer is shown of Fig. 5(c). The SH power vs. the analyzing angle obtained for collecting angle $\gamma = \pi/8$ is plotted on Fig. 5(d). The experimental extinction ratio E_r is ~ 0.5 , while the expected value from the calculations from the same collecting angle is 0.052. This disagreement can be connected with induced nonlinear depolarization of the SH signal that can take place at the strong fundamental field intensity due to self-focusing at GW/cm^2 intensity-level. Additional experiments are needed to confirm this hypothesis.

When the fundamental beam propagates in the direction slightly different from the normal to the z-axis, we observe an interesting behavior of the plane SH radiation at high input powers. Namely, we record a strong bending of the SH light propagating in the close proximity to the fundamental beam. This effect, shown in detail in Fig. 6, is caused by a local effective thermal lens induced by the fundamental beam which bends the trajectory of the generated SH signal. The

images show the front SH emission with the fundamental beam blocked. We notice that the SH divergence increases with the input power. This is a result of the increased divergence of the fundamental beam due to self-focusing.

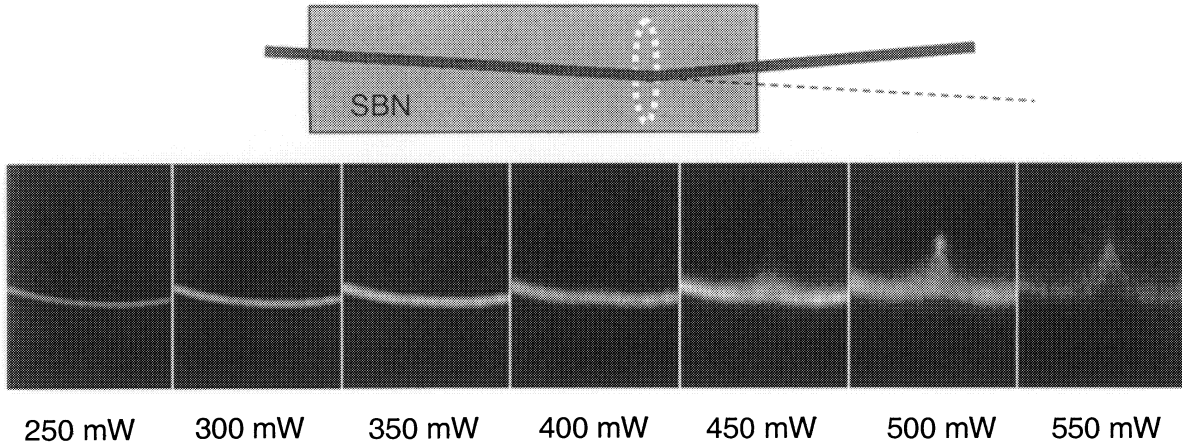


Fig. 6. Modification of the SH radiation in the planar geometry for increasing values of the input power of the fundamental beam..
Top: schematic of the interaction geometry that shows the effect of the effective induce thermal lens.

3. CONCLUSION

We have studied experimentally the femtosecond noncollinear self-phase-matched SHG process in an unpoled SBN crystal with random ferroelectric domains. We have demonstrated that the effect of thermal self-focusing of the fundamental beam has a strong effect on the process of the femtosecond frequency doubling in such SBN crystals. The formation of a thermal nonlinear lens leads to a significant (four-fold) increase of the conversion efficiency, and it results in increasing the spectral width and decreasing a conical angular divergence of the generated second-harmonic signal.

Acknowledgements. Solomon Saltiel and Alexander Dreischuh thank the Nonlinear Physics Centre at the Australian National University for a warm hospitality during their stay in Canberra and acknowledge a support from the National Science Fund (Bulgaria) through the grants F2101/2002 and WUF-02/2005. Solomon Saltiel thanks A.S. Chirkin and A. Arie for stimulating discussions. This work has been supported by the Australian Research Council.

REFERENCES:

1. A.R. Tunyagi, M. Ulex, and K. Betzler, "Noncollinear optical frequency doubling in Strontium Barium Niobate," *Phys. Rev. Lett.* 90, 243901 (2003).
2. R. Fischer, S.M. Saltiel, D.N. Neshev, W. Krolikowski, and Yu.S. Kivshar, "Broadband femtosecond frequency doubling in random media," *Appl. Phys. Lett.* 89 (2006) in press.
3. J.J. Romero, C. Arago, J.A. Gonzalo, D. Jaque, and J. Garcia Sole, "Spectral and thermal properties of quasi-phase-matchingsecond-harmonic generation in $\text{Nd}^{3+}:\text{Sr}_{0.6}\text{Ba}_{0.4}(\text{NbO}_3)_2$ multi-self-frequency-converter nonlinear crystals," *J. Appl. Phys.* 93, 3111-3113 (2003).
4. M. Sheik-Bahae, D.C. Hutchings, D.J. Hagan, and E.W. Van Stryland, "Dispersion of bound electronic nonlinear refraction in solids," *IEEE J. Quantum Electron.* 27, 1296-1309 (1991).